QUARTERLY JOURNAL OF THE ROYAL METEOROLOGICAL SOCIETY
Q. J. R. Meteorol. Soc. **133**: 1589–1604 (2007)
Published online 13 August 2007 in Wiley InterScience
(www.interscience.wiley.com) DOI: 10.1002/qj.119

RMetS
ROYAL METEOROLOGICAL SOCIETY

Stability and accuracy of the physics – dynamics coupling in spectral models

P. Termonia* and R. Hamdi
Royal Meteorological Institute, Brussels, Belgium

ABSTRACT: This article first reviews the existing spectral time-step organizations of the Integrated Forecast System (IFS) of the ECMWF and the ARPEGE/ALADIN/AROME models of Météo-France and the ALADIN partners. They are characterized according to four choices concerning the physics – dynamics coupling: (1) the order in which the physics parametrization and the dynamics are called and coupled inside the time-step computation, (2) the space-time location of the physics coupling on the semi-Lagrangian trajectory, (3) parallel or sequential time stepping of the different physics parametrizations and (4) parallel or sequential physics – dynamics coupling. It is found that according to this classification, IFS on the one hand and the ARPEGE/ALADIN/AROME models on the other hand exhibit two distinct structures.

In the models, the dynamical cores of the semi-implicit semi-Lagrangian two-time-level schemes are linearized around a stationary reference state. This state differs from the real atmospheric state (i.e. the exact solution of the equations). This article generalizes the framework introduced by Staniforth, Wood and Côté to study the relation between the coupled physics parametrization and such reference and atmospheric states. Subsequently, the two above-mentioned time-step organizations are translated into this simplified frame. Extra degrees of freedom are added to allow for obvious improvements of the existing spectral time-step organizations. In order to deal with the complexity of the emerging structures and to avoid tedious algebraic manipulations, a numerical methodology is proposed to characterize their properties. This framework is then used to make a comparative study of the numerical stability and the accuracy of the physics – dynamics coupling within the two above-mentioned time-step organizations. Potential improvements are briefly discussed. Copyright © 2007 Royal Meteorological Society

KEY WORDS numerics; physics parametrization; forced response

Received 6 November 2006; Revised 6 March 2007; Accepted 16 April 2007

1. Introduction

Two distinct approaches can be identified in which the physics – dynamics coupling is accommodated into the time-step organization of spectral semi-implicit semi-Lagrangian (SISL) numerical weather prediction (NWP) models used by the European Centre for Medium-Range Weather Forecasts (ECMWF) and by the ALADIN partners. The first option is the Semi-Lagrangian Averaging of Physical Parametrization (SLAVEPP) scheme (Wedi, 1999) that was developed for the global Integrated Forecast System (IFS) of ECMWF. The second approach is the one of the global ARPEGE model of Météo-France and its related limited-area model ALADIN (ALADIN International team, 1997) of the ALADIN partners, and more lately in the newly developed non-hydrostatic AROME model of Météo-France. The latter models shall be referred to below as the AAA models. The two structures came into use based on different rationales, and have since then equally successfully served their function.

There are two levels at which the numerical stability and the accuracy of the physics-dynamics coupling are realized. The first level is by choosing an appropriate place of the physics – dynamics coupling with respect to the spectral algorithm of the dynamical core in the time-step computation. Numerous examples have been tested in a simplified context, see for instance the seminal paper of Staniforth *et al*. (2002a; referred to as SWC02a henceforth). The second level is in the physics parametrization itself by applying split-implicit schemes.

Wedi (1999) describes the architecture of the SLAVEPP structure. The upshot of this reorganisation of the algorithmics with respect to the older version was a closer approximation of the ideal of second-order accuracy. However, the utilized fractional time stepping, and plugging the coupling between the explicit part of the dynamics and the spectral Helmholtz solver, makes the physics parametrization more linked to the dynamics. One could argue that this complicates the code maintenance, especially in the case of a multiple number of integrated codes having to be maintained in an international collaboration.

In the AAA models, the emphasis has been put on maintenance. Having a physics – dynamics coupling that is entirely separated from the dynamics part of the model,

* Correspondence to: P. Termonia, Royal Meteorological Institute, Ringlaan 3, Brussels, B-1180, Belgium. E-mail: piet.termonia@oma.be

where each physics parametrization is computed independently of the others, allows for a more transparent handling of the code. The argument on accuracy is that many physics parametrizations are first-order accurate anyway. The main emphasis is then on numerical stability, and it has been assumed that this can be controlled inside the parametrizations by using appropriate numerics such as Gaussian elimination for vertical diffusion and split-implicit solutions.

Until now, most of the numerical stability has been realized inside the physics parametrization. The work in SWC02a suggests that, besides accuracy, one may also expect a substantial impact on the stability from a time-step reorganization. However, at present nothing is known with respect to the structure of the time step as imposed by the spectral nature of the models nor of its impact in the 3D models.

Within the AAA modelling context, the non-hydrostatic dynamical core of the ALADIN model (Bubnová *et al*., 1995), referred to as ALADIN-NH, has been selected to become the dynamical core of the new limited-area model AROME of Météo-France. The structure of the time-step organization is essentially copied from the ALADIN model. However, the physics parametrization is now replaced by the parametrization of the meso-NH model (Lafore *et al*., 1998), where no effort comparable to the ARPEGE/ALADIN one was made to stabilize the numerics of the physics parametrizations, creating a situation where the physics determines the time step. This means that it is presently pertinent to revisit this problem while addressing the logical question: 'can the coupling of meso-NH physics to ALADIN-NH dynamics benefit from a reorganization of the time step in the AAA framework?'.

Of course, reorganizing the time step in the AAA models to allow selection of both mentioned structures, or simplifications thereof, would represent a substantial undertaking, the main difficulty being a careful implementation of appropriate physics – dynamics interfaces (e.g. Catry *et al*., 2007) to allow for a modular exchange of the physics packages from one place to another in the code. Our aim is to partially answer the question already as to whether this may be useful, by relying on the generalized method introduced in SWC02a. The present paper will extend this methodology to incorporate the relevant issues imposed by the spectral nature of the models and apply them to retrieve the properties of the currently existing schemes. The emphasis will be put on the organization of the time step and less on the details of the calling sequence of the physics, as is done for instance in Dubal *et al*. (2006). The search for improvements of the existing schemes will be postponed for a subsequent publication.

This paper is organized as follows. The two existing structures of the time step in IFS and the AAA models are first discussed and reduced to their essence as much as possible in Section 2. In Section 3, the generalized framework introduced in SWC02a is extended to include the pertinent features of spectral models and also to consider the interaction between the physics – dynamics coupling and the real atmospheric state. This extended framework is then used to make a comparative study of the stability and the accuracy of the two structures in Section 4. Finally, in Section 5 a summary of the results is presented.

2. The organization of the time step

The two existing structures of the time step in SLAVEPP and the AAA models are first discussed and reduced to their essence as much as possible.

2.1. SLAVEPP

In SLAVEPP, second-order accuracy was aimed at by developing a scheme that approximates the form (Grabowski and Smolarkiewicz, 1996)

$$P^{\frac{1}{2}} = \frac{1}{2}\left(P_{\mathrm{A}}^{+} + P_{\mathrm{D}}^{0}\right), \tag{1}$$

where P denotes the tendency of the physics parametrization, 0 and + represent the t and $t + \Delta t$ time levels, and A and D the arrival and the departure points of the SL trajectory. This represents an averaging along the SL trajectory. The structure of the time step in a semi-implicit spectral model puts two restrictions on the possibilities of realizing this.

Ideally P_{A}^{+} should be included in the formulation of the Helmholtz equation. However, this ideal, which has been referred to as the 'holy grail' by McDonald (1999), is impossible to attain. In order to circumvent this impossibility, it was chosen to make a provisional first-guess prediction of the dynamics at $t + \Delta t$, denoted by $\tilde{F}^{+}$ and use this to compute P_{A}^{+}, following Hortal (1991). This first guess of F^{+} is computed as the adiabatic explicit part of the dynamics plus a correction by half of the linearized dynamics tendency taken at the arrival point, but at t instead of $t + \Delta t$. In the time-step organization, the computation of the physics is thus placed after the computation of the explicit part of the dynamics. The physics is coupled to the dynamics at the arrival point.

In order not to call the physics twice during the time step, the physics of the previous time step is stored in memory, interpolated to the departure point and then used as a P_{D}^{0}. Together with P_{A}^{+}, this then constitutes $P^{1/2}$ in Equation (1).

In fact, due to some encountered instabilities (Wedi, 1999), this time averaging of the physics is only applied for radiation, convection and cloud physics. Vertical diffusion and gravity-wave drag parametrization are treated in a first-order accurate approximation by using their tendency $P_{\mathrm{vert.diff.}}^{+} + P_{\mathrm{g.w.d.}}^{+}$ at $t + \Delta t$ only.

The ECMWF model uses fractional time stepping (Beljaars *et al*., 2004), i.e. fields are updated process by process and serve as input for the subsequent processes. In order to avoid time dependency of the intermediate

DOI: 10.1002/qj

Table I. The different computational steps of interest carried out during the time-step computation of the SLAVEPP structure of the ECMWF model. The one-dimensional symbols of the extended Staniforth – Wood – Côté framework are given in the right column; the updated fields are given instead of the tendencies, except in the case of T_D.

	Computation	1D equivalent
1	Inverse FFT, inverse Legendre transformation	
2	Compute the linear terms	
3	Compute departure point D	
4	Interpolate to D	F_{D}^{*}
5	Explicit part dynamics	$F_{\mathrm{A}}^{\mathrm{exp}}$
	and first-guess correction taken at the arrival point and time t	$\widetilde{F}^{+}$
6	Interpolate diabatic tendencies of radiation, convection and cloud at t to **D**	T_{D}
7	Call physics in a fractional manner	G_M^{exp}
8	Add tendencies of adiabatic and diabatic processes	F^{gp}
9	Direct FFT, direct Legendre transformation	
10	Helmholtz, horizontal diffusion	$F_{\mathrm{A}}^{\mathrm{dyn}}$

time levels, some predictors for F^{+} were used by the physics parametrization, to get what is called 'full fractional stepping'. It should be noted that various technical and scientific constraints determined the specific choice of the predictors. Their current form has been empirically adapted and is inspired by the results.

As such the SLAVEPP scheme represents a feasible compromise to approximate Equation (1) as much as possible. A list of the aspects of the time-step computation that are relevant for the present study is presented in Table I. Note that the physics are computed after the explicit dynamics.

2.2. AAA

In the case of the AAA models, second-order accuracy was not opted for. Instead the physics computation and the coupling to the dynamics is entirely separated from the dynamics computation. In this spirit it is not an option to place the coupling after the computation of the explicit part of the dynamics, so the only possibility is to place it before.

Table II. Similar to Table I, but showing the computational steps carried out during the time-step computation in the AAA models.

	Computation	1D equivalent
1	Inverse FFT, inverse Legendre transformation	
2	Call physics in a parallel manner	ϕ_α
3	Update tendencies	F_{A}^{*}
4	Compute departure point D	
5	Interpolate to D	F_{D}^{*}
6	Explicit part dynamics	$F_{\mathrm{A}}^{\mathrm{exp}}$
7	Direct FFT, direct Legendre transformation	
8	Helmholtz, horizontal diffusion	$F_{\mathrm{A}}^{\mathrm{dyn}}$

This philosophy is extended to the physics calls themselves. Each is computed independently from the others, and all of them coupled separately; the fields are updated by adding the sums of their tendencies. These updated fields are then input to the dynamics computations.

The physics computations are computed at the grid points, the fields are updated and then interpolated to the departure points. So effectively the physics that are input to the dynamics are taken at the departure points. The different computational steps carried out during the time-step computation in the AAA models are presented in Table II.

2.3. Identifying the potential choices

Due to their vertical nature, the physics parametrizations should be computed when the fields are present in grid-point representation. During this part also the explicit part of the dynamics is computed, so there is some freedom to put the physics computation and coupling either before or after it.

The following choices can be identified in the existing model structures. (Categorizing the different possibilities in the time-step organization according to the first three bullet points was suggested to us by J.-F. Geleyn.)

- Coupling of the physics parametrization before or after the explicit part of the dynamics,
- Coupling of the physics to the dynamics at different positions (in space and time) on the SL trajectory,
- Computing the individual physics parametrizations in a parallel or a fractional manner, and
- Coupling the physics to the dynamics by updating the model state and using this for the dynamics, or computing the physics and the dynamics tendencies separately and adding them to get the update; in other words, treat the physics/dynamics in a parallel or a fractional manner.

DOI: 10.1002/qj

The last point is clearly distinct from the previous one. Similarly, as two physics parametrizations can be treated in a sequential or a parallel way, the same can be done for the entire physics parametrization and the explicit part of the dynamics.

Interestingly, both above-mentioned time-step organizations have made exactly the opposite choice.

3. Methodology and first results

3.1. The enhanced canonical problem of the Staniforth – Wood – Côté framework

The proposed one-dimensional equation

$$\frac{\partial F}{\partial t} + U\frac{\partial F}{\partial x} + \mathrm{i}\omega F = -\sum_{\alpha=1}^{N-p} \beta_\alpha F + \sum_{\alpha=p+1}^{N} R_\alpha \, \mathrm{e}^{\mathrm{i}(kx+\Omega_\alpha t)}, \qquad (2)$$

introduced in SWC02a as an extension of the work by Caya *et al.* (1998), is interpreted as follows. The first term on the right-hand side of (2) represents a sum of relaxation processes and the second term represents a sum of oscillatory forcings (with R_α the forcing amplitude, k the wave number and Ω_α the frequency). The spatial coordinate x is taken along a horizontal slice of the atmosphere. The complex $F(x,t)$ is the field obtained after the decomposition of the original fields according to (for instance) a normal-mode decomposition. One may think of this as remaining after the dependence and its vertical differential operators have been factorized; for instance, vertical derivatives are replaced by

$$\frac{\partial}{\partial z}\mathrm{e}^{\mathrm{i}mz} = \mathrm{i}m\,\mathrm{e}^{\mathrm{i}mz}.$$

The left-hand and the right-hand sides of Equation (2) represent the dynamical part and the physics parametrization part of the simplified model, respectively. There is a constant advection U, and the term with ω induces an oscillatory mode that may represent a gravity wave solution of the dynamical part.

It is assumed that $\beta_\alpha \geq 0$. Equation (2) has four types of exact solutions. Table III shows them for the case where there is only one relaxation process and one oscillatory forcing present (the subscript α has been dropped). The solution in the table can be combined to obtain the complete solutions, see SWC02a.

The exact solution will be considered as a reference. For a temporally discretized version with time interval Δt, the time dependence is only sampled without aliasing if

$$-\pi < \Omega\Delta t \leq \pi\,, \quad -\pi < (\omega + kU)\,\Delta t \leq \pi. \qquad (3)$$

Without loss of generality this study will be restricted to $kU \geq 0$.

Von Neumann's method will be used for stability analysis, i.e. the amplification factor $\mathcal{A}$ defined by $F(x, t+\Delta t) = \mathcal{A}\,F(x,t)$ is computed and the stability condition is that $|\mathcal{A}|$ is smaller than 1.

In the current situation, the dynamical core of the IFS/AAA models can be considered as established. So the question posed here will be to take the numerical part of the dynamics in (2) for granted and plug in the physics parametrization at different steps of the time-step organization. So mimicking NWP practice, we first establish the treatment of the dynamics of the canonical problem. This corresponds to $\beta_\alpha = 0$ and $R_\alpha = 0$. In this case the solution is

$$F^{\mathrm{dyn}}(x,t) = \mathrm{e}^{\mathrm{i}\{kx-(\omega+kU)\}t}\,F^{\mathrm{dyn}}(x,0).$$

The methodology in SWC02a is limited to two-time-level (2-TL) SISL schemes.

SI schemes (Robert, 1969) in NWP applications are designed by defining a reference atmospheric state and linearizing the equations around this state. The equations are then expressed as this linearized part and a nonlinear residual. The linearized part is treated in a centred implicit manner, while the residual is treated explicitly. To take this into account, an extension of the scheme in SWC02a,

$$\frac{F_{\mathrm{A}}^{+} - F_{\mathrm{D}}^{0}}{\Delta t} + \frac{\mathrm{i}}{2}\omega^{*}(F_{\mathrm{A}}^{+} + F_{\mathrm{D}}^{0}) + \frac{\mathrm{i}}{2}(\omega - \omega^{*})(F^{(0)} + F_{\mathrm{D}}^{0}) = 0, \qquad (4)$$

will be considered here. The last term expresses the fact that the atmospheric state (quantified by ω) may differ from the reference state (quantified by ω^{*}), as

Table III. The different exact solutions of the equations of the enhanced canonical problem of the Staniforth – Wood – Côté framework.

Name	Expression	Condition
Free solution	$F(x,t) = F_k^{\mathrm{free}}\mathrm{e}^{-\beta t}\mathrm{e}^{\mathrm{i}\{kx-(\omega+kU)t\}}$	$R = 0$
Forced regular solution	$F(x,t) = \dfrac{R}{\beta + \mathrm{i}(\omega + kU + \Omega)}\mathrm{e}^{\mathrm{i}(kx+\Omega t)}$	$\beta + \mathrm{i}(\omega + kU + \Omega) \neq 0$
Forced resonant solution	$F(x,t) = R\,t\,\mathrm{e}^{\mathrm{i}(kx+\Omega t)}$	$\beta = 0$ and $\omega + kU + \Omega = 0$
Forced steady state	$F(x,t) = \dfrac{R\,\mathrm{e}^{\mathrm{i}kx}}{\beta + \mathrm{i}(\omega + kU)}$	$\Omega = 0$ and $F^{\mathrm{free}} = 0$ or $\beta > 0$

DOI: 10.1002/qj

was first studied by Simmons *et al.* (1978). The 1D field $F^{(0)}$ is a guess of F_{A}^{+}. The cases treated in SWC02a can be retrieved by taking $\omega = \omega^*$, assuming that the atmospheric state is equal to the linearization.

In the non-extrapolating scheme, the guess field is chosen as

$$F^{(0)} \equiv F_{\mathrm{A}}^{0}. \tag{5}$$

This corresponds to the 2-TL scheme in Bénard (2003), with one iteration, and mimics the way it has been coded in the AAA models. As stated in that paper, in practical applications the more accurate extrapolating scheme

$$F^{(0)} = 2F_{\mathrm{A}}^{0} - F_{\mathrm{A}}^{-} \quad \text{with} \quad F^{-} \equiv F(t - \Delta t),$$

is used. However, this would render the present stability analysis to one of an effective 3-TL system. Since it is not the aim of this paper to extend the approach in SWC02a to 3-TL, this will not be considered here.

For the non-extrapolating scheme (5) the condition for stability, $|\mathcal{A}| \leq 1$, becomes

$$\left(\omega^* - \omega\right)\left\{\frac{1}{2}\omega\Delta t\,(1 + \cos kU\,\Delta t) + \sin kU\,\Delta t\right\} \geq 0. \tag{6}$$

This paper will restrict itself to $\omega \geq 0$. Then stability is ensured if

$$\omega^* \geq \omega, \tag{7}$$

for all ω, i.e. the reference state should be chosen larger than the frequency of any possible atmospheric mode.

This presence of ω^* is convenient for the present application of the framework, since the discretization of the dynamics is now quantified by ω^*, which will allow the study of the stability of the physics – dynamics coupling with respect to the 'taken-for-granted' dynamics. This extension of the Staniforth – Wood – Côté (SWC) framework, will allow the study of the interaction of the physics-dynamics with the atmospheric state.

In order to gain some understanding of this interaction, it is useful to consider the simple case of an explicit coupling where the problem can be treated analytically. Later in the paper, this will be extended to the structure of the spectral models. A general explicit coupling of a diffusive process,

$$\frac{F_{\mathrm{A}}^{+} - F_{\mathrm{D}}^{0}}{\Delta t} + \frac{\mathrm{i}}{2}\omega^*(F_{\mathrm{A}}^{+} + F_{\mathrm{D}}^{0}) + \frac{\mathrm{i}}{2}(\omega - \omega^*)(F_{\mathrm{A}}^{0} + F_{\mathrm{D}}^{0}) = -\beta F_{\mathrm{D}}^{0}, \tag{8}$$

is stable provided $\beta \leq \beta_{\max}$, with

$$\beta_{\max}\Delta t = 1 - \frac{1}{2}\left(\omega^* - \omega\right)\Delta t \sin kU\,\Delta t + \frac{1}{2}\{4 + 2\omega\left(\omega^* - \omega\right)\Delta t^2\,(1 + \cos kU\,\Delta t) + \left(\omega - \omega^*\right)^2\Delta t^2 \sin^2 kU\,\Delta t\}^{\frac{1}{2}}, \tag{9}$$

which depends on the difference between the atmospheric state and the reference, and also on U due to the approximation of the guess in (5). Note that in the case $\omega = \omega^*$, the result $\beta_{\max}\Delta t = 2$ for the explicit case in SWC02a is retrieved. For calm situations ($U = 0$), choosing a large background has the effect of relaxing the stability condition, i.e. $\beta_{\max}$ increases. On the other hand, for stronger winds, the conditions actually becomes more restrictive, as can be seen from Figure 1, where five cases are shown for $\omega^*\Delta t = 1$ and different values of $\omega\Delta t$. It shows that, for $kU\,\Delta t = \pi/2$, $\beta_{\max}\Delta t$ decreases with decreasing $\omega\Delta t$. This simple example shows that the difference between the linearized and the atmospheric state has an impact on the physics – dynamics coupling and may even make the stability conditions more severe depending on the situation.

Equation (4), as explained above, represents our established dynamical core in the SWC framework. The coupling of the physics to the dynamics is done by adding the physics tendencies

$$F^{\mathrm{C}} = F + \Delta t \sum_{\alpha} \frac{\Delta P_{\alpha}}{\Delta t}, \tag{10}$$

either by updating the fields, i.e. storing F^{C} in F^0 in (4), which is then used to compute the dynamics, or by coupling F^{C} in a parallel manner to the result of the dynamics taking $F^{+} + F^{\mathrm{C}}$ as the result of the time-step computation.

The physics can either be computed in a parallel or a fractional manner. Translated to the SWC framework, the parallel calling order gets the form,

$$\frac{G_\alpha - F}{\Delta t} = \phi_{\mu_\alpha,\alpha}[F, G_\alpha] = \mu_\alpha\phi_\alpha[G_\alpha] + (1 - \mu_\alpha)\,\phi_\alpha[F], \quad \alpha = 1, \ldots, M, \tag{11}$$

with M physics calls, generically denoted by ϕ_α and labelled by the index α. The physics can have either the form

$$\phi_\alpha[F] = -\beta_\alpha F \quad \text{or} \quad \phi_\alpha[F] = R_\alpha \mathrm{e}^{\mathrm{i}[kx + \Omega_\alpha t]}.$$

In the latter case it is understood that

$$\phi_\alpha[G_\alpha] = R_\alpha \mathrm{e}^{\mathrm{i}\{kx + \Omega_\alpha(t + \Delta t)\}} \text{ and } \phi_\alpha[F] = R_\alpha \mathrm{e}^{\mathrm{i}(kx + \Omega_\alpha t)}.$$

The input of the physics calls is F and the output is G_M. The parameter μ_α determines the degree of implicitness of the physics parametrization. Each of the parametrizations is computed independently, and the coupling to the dynamics is done by adding the tendencies $\Delta P_\alpha = G_\alpha - F$, as in (10).

In the SLAVEPP scheme, the physics are computed in a fractional manner. The above-mentioned subtleties concerning the computation of the vertical diffusion and gravity-wave drag will be ignored in the article. The

DOI: 10.1002/qj

definition will be reduced to that of the sequential physics as in Dubal *et al*. (2004),

$$\frac{G_\alpha - G_{\alpha-1}}{\Delta t} = \phi_{\mu_\alpha,\alpha}[G_{\alpha-1}, G_\alpha] = \mu_\alpha \phi_\alpha[G_\alpha] + (1-\mu_\alpha)\,\phi_\alpha[G_{\alpha-1}], \quad G_0 \equiv F; \quad \alpha = 1, \ldots, M, \tag{12}$$

with notation similar to (11). In this case there is only one tendency $\Delta P_1 = G_M - F$ to be coupled in (10).

Note that the Δt dependence of the discretized equations can be completely absorbed into dimensionless parameters,

$$\widetilde{U} \equiv kU\Delta t, \quad \widetilde{\omega} \equiv \omega \Delta t, \quad \widetilde{\beta}_\alpha \equiv \beta_\alpha \Delta t, \quad \widetilde{R}_\alpha \equiv R_\alpha \Delta t, \quad \widetilde{\Omega}_\alpha \equiv \Omega_\alpha \Delta t. \tag{13}$$

The point of view taken here is that of the AAA structure and to see whether an adaptation to the SLAVEPP structure can lead to substantial benefits. In this sense it is not our aim to exactly mimic the SLAVEPP structure, but to approach it sufficiently closely in the simplified set-up.

3.2. Where to couple on the SL trajectory?

One of the four choices that can be made is where to couple on the SL trajectory. It is first investigated in the simplest possible model, without ω-forcing but with only a diffusive relaxation. The point on the trajectory for the solution of the form $F(x,t) = f(t)\,\mathrm{e}^{\mathrm{i}kx}$ is determined by

$$F(A - U\lambda\Delta t, t) = \mathrm{e}^{-\mathrm{i}\lambda kU\Delta t} F(A,t), \tag{14}$$

where λ locates the point with respect to the arrival point A corresponding to $\lambda = 0$ and the departure point D corresponding to $\lambda = 1$. For $\lambda \neq 0$, this can be considered to represent the interpolation back along the SL trajectory

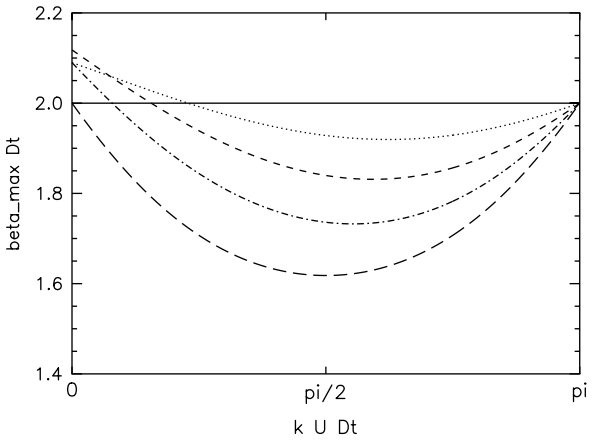

Figure 1. The maximum value $\beta_{\max}\Delta t$ for conditional stability, as a function of the dimensional parameter $kU\Delta t$ (see text for explanation), for a diffusive process coupled to the dynamics with $\omega^*\Delta t = 1$ for different choices $\omega = \omega^*$ (solid line), $\omega = 0.75\,\omega^*$ (dots), $\omega = 0.5\,\omega^*$ (short dashes), $\omega = 0.25\,\omega^*$ (dash dot), $\omega = 0$ (long dashes).

of a physics parametrization tendency that has been computed along the vertical on a grid point.

In the case of an explicit coupling of a diffusive process

$$\frac{F(A, t+\Delta t) - F(D,t)}{\Delta t} = -\beta\,\mathrm{e}^{-\mathrm{i}\lambda kU\Delta t} F(A,t), \tag{15}$$

the condition for stability becomes

$$\beta\Delta t \leq 2\cos(1-\lambda)kU\Delta t, \tag{16}$$

which generically depends on the scale of the mode and the advection; in the case $(1-\lambda)kU\Delta t = \pi/2$ the scheme is unstable. The only way to avoid this is to take $\lambda = 1$, i.e. couple the physics at the departure point.

Analogously, in the case of an implicit treatment

$$\frac{F(A, t+\Delta t) - F(D,t)}{\Delta t} = -\beta\,\mathrm{e}^{-\mathrm{i}\lambda kU\Delta t} F(A, t+\Delta t), \tag{17}$$

the stability condition is

$$\beta\Delta t \geq -2\cos\lambda kU\Delta t, \tag{18}$$

which now becomes independent from k and U if $\lambda = 0$, i.e. if the parametrization is coupled at the arrival point.

Since turbulent vertical diffusion is always present in the models, the above instabilities should be avoided at all costs. In fact, the conditions on λ correspond to where the air parcel is on the SL trajectory for the respective times. From these cases, we propose to generalize the stability analysis in SLAVEPP (Wedi, 1999; J.-F. Geleyn, personal communication) to a synthesizing guidance rule for the modeller inserting a new physics parametrization into the time step: *the physics parametrization should always be coupled to the air parcel*. Note that this holds for any SL scheme independently of the precise details of the discretization of the model. This rule eliminates one degree of freedom in the four choices in organizing the time step in subsection 2.3.

3.3. Extension of the SWC framework to spectral models

The SWC framework can easily be translated to spectral models. The pth-order derivatives are replaced by multiplication with the wave numbers $(\mathrm{i}k)^p$ without having to specify the spectral transform in detail. In the SWC framework, all equations can be solved analytically. For instance, solving the Helmholtz equations is reduced to a multiplication with the implicit operator $(1 + \mathrm{i}\omega^*\Delta t/2)^{-1}$. Although the nature of the equations does not impose constraints on the numerics as in the realistic models, the consequential algorithmic choices will be translated into the enhanced canonical problem.

Tables IV and V show the above introduced aspects of the time-step computation in the SWC framework for two structures corresponding to parallel and sequential physics parametrization calls. In fact, these represent

DOI: 10.1002/qj

Table IV. Simplified model frame for parallel interfaces based upon the structure of the model codes of the AAA models. The acronyms in the left column denote the type of space, spectral (SP) or grid-point (GP), in which the computation is performed.

SP	Derivatives	$\partial_x^p F_\mathrm{A} = (\mathrm{i}k)^p F$
Inverse spectral transform		
	Physics (level I)	$\dfrac{G_\alpha - F_\mathrm{A}^0}{\Delta t} = \xi_\alpha \phi_\alpha [F_\mathrm{A}^0, G_\alpha], \quad \alpha = 1, \ldots, M$
	Coupling	$F_\mathrm{A}^* = F_\mathrm{A}^0 + \Delta t \sum_{\alpha=1}^{M} \dfrac{G_\alpha - F_\mathrm{A}^0}{\Delta t}$
	Interpolation	$F_\mathrm{D}^* = \mathrm{e}^{-\mathrm{i}kU\Delta t} F_\mathrm{A}^*$
GP	Explicit dynamics	$F_\mathrm{A}^\mathrm{exp} = \left(1 - \dfrac{\mathrm{i}\omega}{2}\Delta t\right) F_D^* - \dfrac{\mathrm{i}}{2}(\omega - \omega^*)\Delta t F^{(0)}$
	Full TL first guess	$\widetilde{F}^+ = F_\mathrm{A}^\mathrm{exp} - \dfrac{\mathrm{i}}{2}\omega^* \Delta t \, F_\mathrm{A}^*$
	Physics (level II)	$\dfrac{G_\alpha^\mathrm{exp} - \widetilde{F}^+}{\Delta t} = (1-\xi_\alpha)(1-\nu_\alpha)\phi_\alpha[\widetilde{F}^+; G_\alpha^\mathrm{exp}]; \ \alpha = 1, \ldots, M$
	Coupling	$G_\mathrm{A}^\mathrm{exp} = \widetilde{F}^+ + \Delta t \sum_{\alpha=1}^{M} \dfrac{G_\alpha^\mathrm{exp} - \widetilde{F}^+}{\Delta t}$
	Subtract first guess	$F^\mathrm{gp} = G_\mathrm{A}^\mathrm{exp} + \dfrac{\mathrm{i}}{2}\omega^* \Delta t \, F_\mathrm{A}^*$
Direct spectral transform		
SP	Implicit dynamics	$F_\mathrm{A}^\mathrm{dyn} = \left(1 + \dfrac{\mathrm{i}\omega^*}{2}\Delta t - \Delta t \sum_{\alpha=1}^{M}(1-\xi_\alpha)\nu_\alpha \phi_\alpha^\mathrm{imp}\right)^{-1} F^\mathrm{gp}$

Table V. Simplified model frame for sequential interfaces based upon the structure of the IFS model. The acronyms in the left column denote the type of space, spectral (SP) or gridpoint (GP), in which the computation is performed.

SP	Derivatives	$\partial_x^p F_\mathrm{A} = (\mathrm{i}k)^p F$
Inverse spectral transform		
	Physics (level I)	$\dfrac{G_\alpha - G_{\alpha-1}}{\Delta t} = \xi_\alpha \phi_\alpha [G_{\alpha-1}, G_\alpha]; \ \alpha = 1, \ldots, M; \ G_0 \equiv F_\mathrm{A}^0$
	Interpolation	$F_\mathrm{D}^* = \mathrm{e}^{-\mathrm{i}kU\Delta t} F_\mathrm{A}^0, \quad T_\mathrm{D} = \mathrm{e}^{-\mathrm{i}kU\Delta t} \dfrac{G_M - F_\mathrm{A}^0}{\Delta t}$
GP	Explicit dynamics	$F_\mathrm{A}^\mathrm{exp} = \left(1 - \dfrac{\mathrm{i}\omega}{2}\Delta t\right) F_\mathrm{D}^* - \dfrac{\mathrm{i}}{2}(\omega - \omega^*)\Delta t \, F^{(0)}$
	Full TL first guess	$\widetilde{F}^+ = F_\mathrm{A}^\mathrm{exp} - \dfrac{\mathrm{i}}{2}\omega^* \Delta t \, F_\mathrm{A}^0$
	Physics (level II)	$\dfrac{G_\alpha^\mathrm{exp} - G_{\alpha-1}^\mathrm{exp}}{\Delta t} = (1-\xi_\alpha)(1-\nu_\alpha)\phi_\alpha[G_{\alpha-1}^\mathrm{exp}, G_\alpha^\mathrm{exp}]; \ \alpha = 1, \ldots, M; \ G_0^\mathrm{exp} \equiv \widetilde{F}^+$
	Coupling	$F^\mathrm{C} = T_\mathrm{D}\Delta t + G_M^\mathrm{exp}$
	Subtract first guess	$F^\mathrm{gp} = F^\mathrm{C} + \dfrac{\mathrm{i}}{2}\omega^* \Delta t \, F_\mathrm{A}^0$
Direct spectral transform		
SP	Implicit dynamics	$F_\mathrm{A}^\mathrm{dyn} = \left\{1 + \dfrac{\mathrm{i}\omega^*}{2}\Delta t - \Delta t \sum_{\alpha=1}^{M}(1-\xi_\alpha)\nu_\alpha \phi_\alpha^\mathrm{imp}\right\}^{-1} F^\mathrm{gp}$

generalizations of the existing time-step organizations in the existing AAA models and IFS model. Indeed, in the real AAA models, the physics are computed and coupled always before the explicit part of the dynamics, corresponding to $\xi_\alpha = 1$. Values different from 1 are included here to allow us to explore reorganizations of the AAA models without reorganizing the order of the calls within the physics computation package. Likewise, the SLAVEPP scheme in Wedi (1999) corresponds to $\xi_\alpha = 0.5$. So within the SWC framework the acronyms AAA and IFS will actually refer to this broader class of time-step organizations. The embedding of the existing models within this generalization will be discussed in more detail below.

Following what is done in the studied IFS and AAA models, in Tables IV and V the 'established' dynamics are split into an explicit part (computed in the grid-point part of the time step) and the inverse of the implicit

DOI: 10.1002/qj

operator (computed in the spectral part of the time step). Indeed, in the case of no physics coupling, $\phi_\alpha = 0$, this reduces to the dynamics as in Equation (4).

The physics parametrization in Equations (11) and (12) can then be called before or after the explicit part of the dynamics, indicated as level I and level II in the tables. In the case of level II physics, it is necessary to include the above-mentioned first guess of the full time level result as in the SLAVEPP scheme. This is indicated in the tables by 'Full TL first guess' and is denoted by $\widetilde{F}^+$. The physics are then computed using $\widetilde{F}^+$. This has to be corrected again before going to spectral space by 'subtracting the first guess'. In the tables, the physics parametrizations are multiplied with parameters ξ_α determining their position with respect to the explicit dynamics. If the physics are called entirely before the dynamics, i.e. $\xi_\alpha = 1$ as is done in the AAA models, there is no need for the full TL first guess, since the subsequent subtraction cancels it anyway.

The place of the interpolation to the departure point is determined by the dynamics. Note that in the table the rule of coupling to the air parcel is followed. At level I, we are at the time t, the physics are computed on the grid points but interpolated to the departure points as part of the updated field F^*_{A}. At level II, the physics are computed, albeit approximately, at the full time level $t + \Delta t$ and kept at the arrival point. In a model code there exist some freedom as to where to interpolate the tendencies of the physics at time level t. This can be performed before the computation of the explicit part of the dynamics. But since it is not used until the coupling, it could also be done later.

In Tables IV and V, part of the physics is included in the inverse of the implicit operator, parametrized by the parameters ν_α, mimicking the ideal of having the physics treated as part of the Helmholtz solver being called 'the holy grail' by McDonald (1999). This case is included not because of practical interest (see McDonald, 1999; Wedi, 1999 for a discussion), but since it may serve as an ideal reference to which all the other compromise solutions may be compared.

In order to make the comparison with the time-step computations of the realistic models, the 1D symbols of the results in Tables IV and V have been added in Tables II and I respectively.

It should be stressed that rather severe simplifications have been made in Table V compared to the SLAVEPP scheme. The computation of G_α in Equation (12) depends on $G_{\alpha-1}$ only, whereas in the ECMWF model the dependence in the sequential calls may be more complicated. For instance, in Beljaars *et al.* (2004) two options for the vertical diffusion scheme were considered: (i) the diffusion coefficients can be computed from time level 0 or (ii) they are computed from profiles incremented with the dynamics. Also in Table V, P^0_{D} in (1) is computed whereas in the ECMWF model it is taken from the previous time step.

The two levels mentioned in the Introduction, at which we have some freedom for improving the stability and the accuracy of the physics – dynamics coupling, clearly appear in this framework. The first level of the position in the time-step organization is labelled by ξ_α, positioning the computation of physics and the different natures of the physics – dynamics coupling between Tables IV and V. This is determined within the organization of the time step. Secondly, there is the degree of implicitness labelled by μ_α, which in the models is determined inside the physics package, 'below' the physics – dynamics coupling.

By limiting ourselves to a 2-TL scheme, the dependence of F^+ on F^0 remains linear. So, without loss of generality, the amplification can be studied by taking $F^0 = 1$. To study the effect of the physics (parametrized by e.g. $\widetilde{\beta}_\alpha$) on the dynamics, the amplification should be studied as a function of $\widetilde{\omega}^*$ and the parameter of the physics.

In applications, the stability of a model will be determined by the most unstable mode. This corresponds to an existing belief among modellers that if an unstable mode exists, the model will generate it sooner or later. This paper will restrict itself to identifying the most unstable modes. The instability of the model will thus be determined by the largest amplification factor $|\mathcal{A}|$. So the maximum will be taken over the remaining dimensionless parameters $0 \le \widetilde{U} \le \pi$, $0 \le \widetilde{\omega} \le \pi$.

4. Comparing the two time-step organizations

The aim of this section is to study the different physics forcings separately. The approach here is to derive the restrictions on the time step by gradually adding more and more forcing to the physics part of the canonical problem. This will lead to stability requirements additional to Equation (7) and similarly Equation (9) needs to be satisfied when switching on the diffusive forcing in the right-hand side of Equation (8).

As noted by SWC02b, the amount of vertical diffusion can be expected to play an important role in damping spurious amplification of the numerical solution of the freely forced response. Thus a free forcing will be added and the time-step amplification will be studied as a function of $\beta\Delta t$ and the dynamics parameter $\omega^*\Delta t$.

The different splitting steps presented in Tables IV and V may be summarized in symbolic form as:

- AAA:

$$\xi_\alpha \phi^{\alpha,I}_{\mu_{\alpha,I}} \mapsto \mathcal{D}^{\exp} \mapsto (1-\xi_\alpha)(1-\nu_\alpha)\phi^{\alpha,II}_{\mu_{\alpha,II}} \mapsto \mathcal{D}^{\mathrm{imp}} + (1-\xi_\alpha)\nu_\alpha \phi^{\alpha,\mathrm{imp}}. \tag{19}$$

- IFS:

$$\mathcal{D}^{\exp} \mapsto \{(1-\xi_\alpha)(1-\nu_\alpha)\phi^{\alpha,II}_{\mu_{\alpha,II}} + \xi_\alpha \phi^{\alpha,I}_{\mu_{\alpha,I}}\} \mapsto \mathcal{D}^{\mathrm{imp}} + (1-\xi_\alpha)\nu_\alpha \phi^{\alpha,\mathrm{imp}}. \tag{20}$$

DOI: 10.1002/qj

$\mathcal{D}^{\text{exp}}$ represents the computation of the explicit part of the dynamics computed in the grid-point part of the time step, $\mathcal{D}^{\text{imp}}$ and $\phi^{\alpha,\text{imp}}$ stand for the implicit part of the dynamics and the physics respectively computed in the spectral part of the time step and mimicking the ideal of having the physics treated as part of the Helmholtz solver. The superscripts I, II denote the computation of the physics at level I, II respectively and $\mu_{\alpha,I}$ and $\mu_{\alpha,II}$ denote which off-centring weights are associated with the time-weighted-implicit discretization of a specific process α. In the case of only one physics forcing being present, the index α will be omitted from the notation.

4.1. Stability and accuracy of the free solution

4.1.1. Stability

For the free solution, i.e. with one diffusive forcing,

$$M = 1 \text{ (so } \alpha \text{ will not be written);}$$
$$\phi \equiv -\beta F;\ \phi^{\text{imp}} \equiv -\beta,$$

and four special cases of Equations (19) and (20) will be studied, see Table VI. These schemes mimic the time-step organizations of:

(a) SLAVEPP (IFS-imp) with implicit physics parametrization,
(b) the AAA models with implicit physics parametrizations (AAA-imp),
(c) a version of the SLAVEPP structure but with the physics parametrization computed explicitly, representing the case where no effort is made to stabilize the numerics of the physics parametrizations (IFS-exp), and analogously
(d) an AAA-exp model, being the AAA time-step structure but with explicit physics parametrization.

The simplified IFS-imp and AAA-imp are the best representatives of the existing IFS and AAA models.

Our simplified IFS model (Equation (20)) can also approach the 'holy grail' solution sufficiently closely by taking $(\xi, \nu, \mu_I) = \left(\frac{1}{2}, 1, 0\right)$:

$$F_{\text{A}}^{+} = \frac{\left(1 - \frac{\beta\Delta t}{2} - \text{i}\frac{\omega\Delta t}{2}\right)\text{e}^{-\text{i}kU\Delta t} - \frac{\text{i}}{2}(\omega - \omega^*)\Delta t}{1 + \frac{\beta\Delta t}{2} + \text{i}\frac{\omega^*\Delta t}{2}} F_{\text{A}}^{0}. \tag{21}$$

Figure 2 presents the amplification factor $|\mathcal{A}|$ derived from Von Neumann's method as a function of the dynamics discretization, parametrized by $\omega^*\Delta t$, and the amount of diffusion expressed by $\beta\Delta t$, for the four schemes presented in Table VI and for the 'holy grail' solution (Equation (21)).

As is shown in Figures 2(b) and (e), the AAA-imp scheme and the 'holy grail' solution share the advantage of being stable independently of $\omega^*\Delta t$ and up to values of $\beta\Delta t = 10$. For the AAA-imp scheme, the amplification factor $|\mathcal{A}|$ decreases monotonically as a function of $\beta\Delta t$. The IFS-imp scheme on the other hand (Figure 2(a)) becomes unstable for fast damping processes $\beta\Delta t$ and large background $\omega^*\Delta t$. To guarantee that the amplification factor $|\mathcal{A}|$ decreases monotonically, the restrictive condition $\beta\Delta t \leq 2$ should be satisfied.

For Figures 2(c) and (d), which represent the IFS-exp and the AAA-exp scheme respectively, the condition for stability ($|\mathcal{A}| \leq 1$) becomes very restrictive for fast damping processes and large background ($\beta\Delta t \leq 1.2$). To guarantee that the amplification factor $|\mathcal{A}|$ decreases monotonically as the damping coefficient $\beta\Delta t$ increases, the restrictive condition $\beta\Delta t \leq 1$ should be satisfied.

These results suggest that, *in the absence of any external forcing, simply adapting the time-step organization of the AAA models to the one of the IFS model, as was presented here, does not enhance its stability.* It will be shown later in Section 4.3 that, when adding a forced response, one may arrive at the opposite conclusion.

It is well known that fast diffusive processes should be treated implicitly or even over-implicitly. The results for the IFS-imp scheme in Figure 2(a) show that the situation is more subtle. They show that within the IFS schemes, implicitness controlled by setting the parameters $\mu_I = 1$ and $\mu_{II} = 1$ is not sufficient but that it should even be treated in an off-centred manner between level I and level II, as controlled by ξ. Taking $\xi = 1$ leads to a stable scheme with properties as shown in Figure 3, which are identical to ones of the AAA-imp scheme in Figure 2(b). This confirms the choice in the empirically adapted version of the SLAVEPP scheme in the ECMWF model (Beljaars *et al.*, 2004), where vertical diffusion is not averaged along the SL trajectory, but taken at level II only.

4.1.2. Accuracy

Applying a Taylor series expansion in terms of Δt of $F_{\text{A}}^{+} - F_{\text{free}}^{\text{exact}}$ calculated for the AAA (19) and IFS

Table VI. Four schemes to mimic the time-step organization of: (a) SLAVEPP (IFS-imp), (b) the AAA models (AAA-imp), (c) SLAVEPP but with explicit physics parametrizations (IFS-exp), (d) the AAA models with explicit physics parametrizations (AAA-imp).

Value	IFS/AAA	Scheme
$(\xi, \nu, \mu_I, \mu_{II}) = (0.5, 0, 1, 1)$	(a) IFS-imp	$\mathcal{D}^{\text{exp}} \mapsto \frac{1}{2}(\phi_1^I + \phi_1^{II}) \mapsto \mathcal{D}^{\text{imp}}$
$(\xi, \nu, \mu_I) = (1, 0, 1)$	(b) AAA-imp	$\phi_1^I \mapsto \mathcal{D}^{\text{exp}} \mapsto \mathcal{D}^{\text{imp}}$
$(\xi, \nu, \mu_I, \mu_{II}) = (0.5, 0, 0, 0)$	(c) IFS-exp	$\mathcal{D}^{\text{exp}} \mapsto \frac{1}{2}(\phi_0^I + \phi_0^{II}) \mapsto \mathcal{D}^{\text{imp}}$
$(\xi, \nu, \mu_I) = (1, 0, 0)$	(d) AAA-exp	$\phi_0^I \mapsto \mathcal{D}^{\text{exp}} \mapsto \mathcal{D}^{\text{imp}}$

DOI: 10.1002/qj

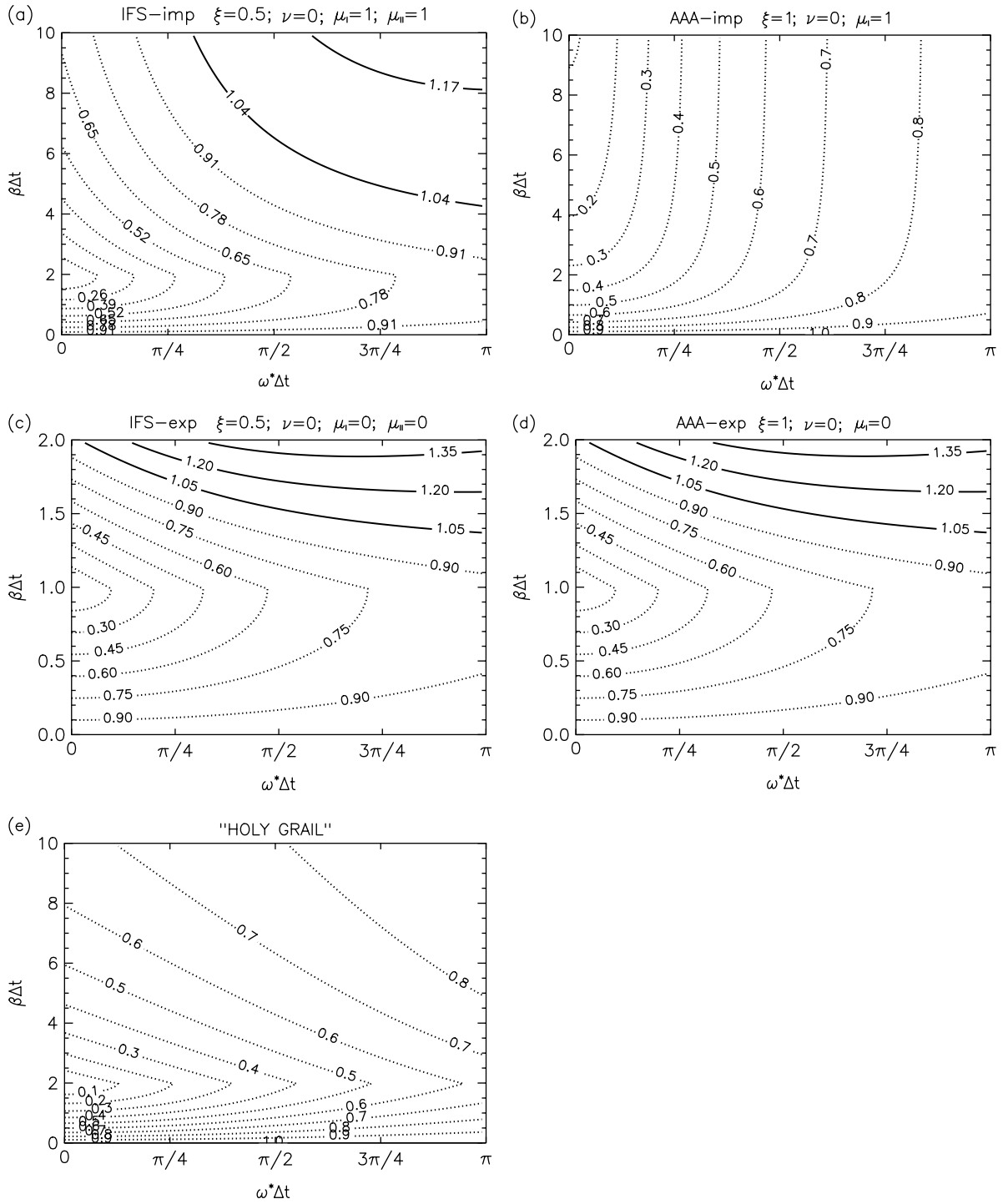

Figure 2. The amplification factor $|\mathcal{A}|$ derived from Von Neumann's method as a function of the dynamics discretization, parametrized by $\omega^*\Delta t$, and the amount of diffusion expressed by $\beta\Delta t$, for the four schemes presented in Table VI and for the 'holy grail' solution.

(20) schemes and assuming that the contribution of the residual part in (4) is zero ($\omega = \omega^*$) leads to

- IFS:

$$F_{\mathrm{A}}^{+} - F_{\mathrm{free}}^{\mathrm{exact}} = \frac{1}{2}\beta F_{\mathrm{A}}^{0}\{\beta[-1 - 2\nu(\xi - 1) + 2\mu_I\xi^2 + 2\mu_{II}(\nu - 1)^2(\xi - 1)^2] + \mathrm{i}\omega(1 - 2\xi)\}\Delta t^2 + O(\Delta t^3). \quad (22)$$

Thus the discrete solution agrees with the exact one to $O(\Delta t)$. However, independently of ω and β, the combination of $(\xi, \nu, \mu_I, \mu_{II})$ that satisfies the simultaneous equations

$$\xi = \frac{1}{2},$$

$$(\nu - 1) + \frac{1}{2}\{\mu_I + \mu_{II}(\nu - 1)^2\} = 0, \quad (23)$$

DOI: 10.1002/qj

increases the accuracy of the discrete solution to $O(\Delta t^2)$. Two situations are of interest:

(i) $(\xi, \nu, \mu_I, \mu_{II}) = \left(\frac{1}{2}, 0, 1, 1\right)$ which corresponds to the IFS-imp case $\mathcal{D}^{\exp} \mapsto \left\{\frac{1}{2}(\phi_1^I + \phi_1^{II})\right\} \mapsto \mathcal{D}^{\text{imp}}$, and

(ii) $(\xi, \nu, \mu_I) = \left(\frac{1}{2}, 1, 0\right)$ which corresponds to the 'holy grail' solution (21).

Note that the decision not to average the vertical diffusion along the SL trajectory in the current SLAVEPP scheme (Beljaars *et al.*, 2004) corresponding to $(\xi, \nu, \mu_{II}) = (0, 0, 1)$ destroys second-order accuracy in (22).

- AAA:

$$F_{\text{A}}^{+} - F_{\text{free}}^{\text{exact}} = \frac{1}{2}\beta F_{\text{A}}^{0}\{\beta[2\mu_{II}(\nu-1)^2(\xi-1)^2 + 2\nu(\xi-1)^2 + 2\xi^2\mu_I - 2\xi(\xi-1) - 1] - \text{i}\omega(\xi-1)\}\Delta t^2 + O(\Delta t^3). \quad (24)$$

Thus, the discrete solution agrees to the exact one to $O(\Delta t)$. However, independently of ω and β, the combination $(\xi, \mu_I) = \left(1, \frac{1}{2}\right)$ increases the accuracy of the discrete solution to $O(\Delta t^2)$, which corresponds to $\phi_{0.5}^I \mapsto \mathcal{D}^{\exp} \mapsto \mathcal{D}^{\text{imp}}$. However with respect to the fully implicit AAA version ($\xi = 1, \mu_I = 1$), the stability is now reduced to exactly the one of the fully implicit IFS case. This can be seen by closely comparing Figure 4 to Figure 2(a).

This analysis confirms the characteristics of the two existing structures of SLAVEPP and the AAA models as described in the introduction.

4.2. The forced regular response

For the forced regular response

$$M = 2, \qquad \phi^1 \equiv -\beta F, \qquad \phi^2 \equiv R\,\text{e}^{\text{i}(kx+\Omega t)},$$

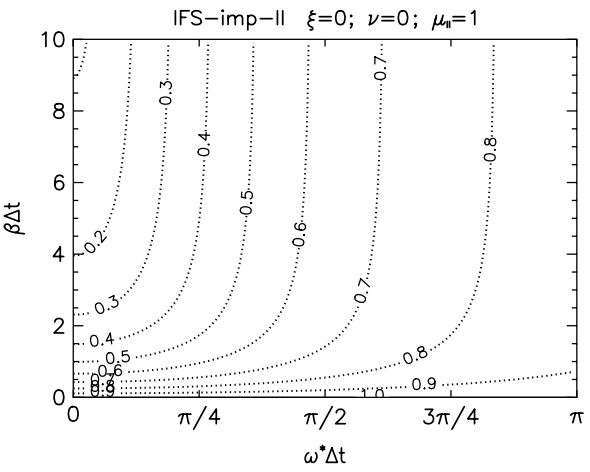

Figure 3. The amplification factor $|\mathcal{A}|$ of the scheme $\mathcal{D}^{\exp} \mapsto \phi_1^{II} \mapsto \mathcal{D}^{\text{imp}}$ with $\phi[F] = -\beta F$.

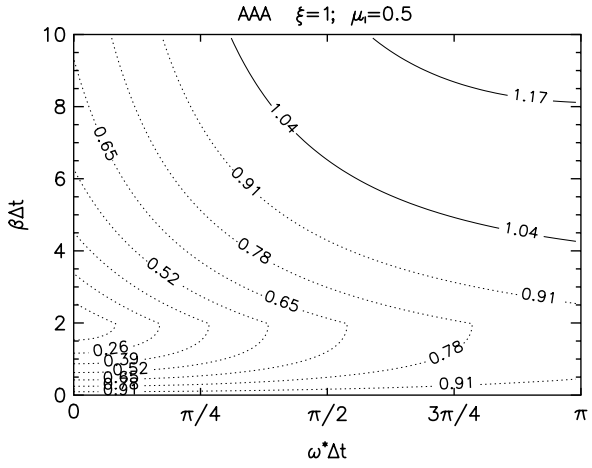

Figure 4. The amplification factor $|\mathcal{A}|$ of the scheme $\phi_{0.5}^I \mapsto \mathcal{D}^{\exp} \mapsto \mathcal{D}^{\text{imp}}$.

$$\phi^{1,\text{imp}} \equiv -\beta, \quad \phi^{2,\text{imp}} \equiv 0, \quad F_{\text{A}}^{0} = \frac{R}{\beta + \text{i}(\omega + kU + \Omega)},$$

and in order to follow the operational environment of IFS and make the analysis more tractable, we assume that $\xi_1 = \xi_2 = \xi$, $\nu_1 = \nu$, and $\nu_2 = 0$.

4.2.1. *Steady-state response.*

If $k \equiv 0$ and $\Omega \equiv 0$, i.e. the forcing is constant, a forced steady-state response exists provided either $F^{\text{free}} = 0$ or $\beta > 0$ holds, and the exact solution (Table III) reduces to

$$F_{\text{steady}}^{\text{exact}} = \frac{R}{\beta + \text{i}\omega}, \quad (25)$$

and a desirable property of any coupling scheme is the ability to reproduce this solution. Any scheme that is unable to correctly represent the steady state is likely to contain systematic errors leading to climate drift. Unfortunately the importance of these errors is difficult to estimate in a general way and may require a case-by-case analysis. So, some estimate is useful of how important they are. This can be done by applying a Taylor series expansion in terms of Δt of the difference between the discrete and the exact solution

$$(\beta + \text{i}\omega)^2 \left(\frac{F_{\text{steady}}^{\text{discrete}}}{R} - \frac{F_{\text{steady}}^{\text{exact}}}{R}\right),$$

where $F_{\text{steady}}^{\text{exact}}$ is taken as in Table III, and where the steady state $F_{\text{steady}}^{\text{discrete}}$ of the discretized scheme is defined by solving the equation $F_{\text{A}}^{\text{dyn}} = F_{\text{A}}^{0}$ for F_{A}^{0}, with $F_{\text{A}}^{\text{dyn}}$ defined as in Tables IV and V.

- IFS: For the IFS step method with its sequential call of the physics, the order in which the physics terms are treated can be important. This can be achieved in a numerical context by using an *a priori* symmetrized sequential-split method as in Dubal *et al.* (2004). If the choice is made to treat $\phi^2 = R$ symmetrized around

DOI: 10.1002/qj

$\phi^1 = -\beta F$, then the calculation of the physics in level I and II (see Table V) can be written:

$$\text{level I} \begin{cases} \dfrac{G_1 - G_0}{\Delta t} = \xi \eta_1 R \\ \dfrac{G_2 - G_1}{\Delta t} = \\ -\beta\xi\{\mu_{1,I} G_2 + (1-\mu_{1,I}) G_1\} \\ \dfrac{G_3 - G_2}{\Delta t} = \xi(1-\eta_1)R, \end{cases} \tag{26}$$

and

$$\text{level II} \begin{cases} \dfrac{G_1^{\exp} - G_0^{\exp}}{\Delta t} = (1-\xi)\eta_2 R \\ \dfrac{G_2^{\exp} - G_1^{\exp}}{\Delta t} = -\beta(1-\xi)(1-\nu) \\ \quad \times\{\mu_{1,II} G_2^{\exp} + (1-\mu_{1,II}) G_1^{\exp}\} \\ \dfrac{G_3^{\exp} - G_2^{\exp}}{\Delta t} = (1-\xi)(1-\eta_2)R. \end{cases} \tag{27}$$

η_1, η_2 determine the symmetry of the scheme.

The accuracy is given by:

$$\begin{aligned} (\beta+\mathrm{i}\omega)^2 \left(\frac{F^{\text{discrete}}_{\text{steady}}}{R} - \frac{F^{\text{exact}}_{\text{steady}}}{R} \right) = \\ \big[\beta^2\{\mu_{1,I}\xi^2 + \mu_{1,II}(\nu-1)^2(\xi-1)^2 \\ - \eta_1\xi^2 + \eta_2(\nu-1)(\xi-1)^2\} \\ + \mathrm{i}\beta\omega\{(\nu-1)(\xi-1) - \eta_1\xi^2 \\ + \eta_2(\nu-1)(\xi-1)^2\}\big]\Delta t + O(\Delta t^2). \end{aligned} \tag{28}$$

Thus, independently of ω and β, if $\nu = 0$ the combination of $(\xi, \mu_{1,I}, \mu_{1,II}, \eta_1, \eta_2)$ satisfying

$$\begin{aligned} (\xi-1) + \mu_{1,I}\xi^2 + \mu_{1,II}(\xi-1)^2 = 0 \\ (\xi-1) + \eta_1\xi^2 + \eta_2(\xi-1)^2 = 0, \end{aligned} \tag{29}$$

reduces all higher-order terms of the Taylor series to zero and thus produces the correct steady-state solution. A number of situations are of interest. A first one is given by $\xi = 0$ and $\eta_2 = \mu_{1,II} = 1$, which is fully implicit, with all ϕ^2 treated before ϕ^1:

$$\mathcal{D}^{\exp} \mapsto \left(\phi^{2,II} \mapsto \phi_1^{1,II}\right) \mapsto \mathcal{D}^{\text{imp}}, \tag{30}$$

where $\phi_1^{1,II}$ means that $\mu_{1,II} = 1$. The stability function of this scheme is the same as the AAA-imp model (Figure 2(b)). A second case of interest is given by $\xi = 1$ and $\eta_1 = \mu_{1,I} = 0$, which is explicit, with all ϕ_2 treated after ϕ_1:

$$\mathcal{D}^{\exp} \mapsto \left(\phi_0^{1,I} \mapsto \phi^{2,I}\right) \mapsto \mathcal{D}^{\text{imp}}, \tag{31}$$

where $\phi_0^{1,I}$ means that $\mu_{1,I} = 0$. A third case is given by $\xi = \frac{1}{2}$, $\eta_1 = \eta_2 = \mu_{1,I} = \mu_{1,II} = 1$ which corresponds to the SLAVEPP case with the same order as given in Wedi (1999):

$$\begin{aligned} \mathcal{D}^{\exp} \mapsto \frac{1}{2}\left\{\left(\phi^{2,II} \mapsto \phi_1^{1,II}\right) + \left(\phi^{2,I} \mapsto \phi_1^{1,I}\right)\right\} \\ \mapsto \mathcal{D}^{\text{imp}}, \end{aligned} \tag{32}$$

and is second-order accurate.

The same results are found if the analysis is made with $\phi^1 = -\beta F$ *a priori* symmetrized around $\phi^2 = R$.

- AAA:

$$\begin{aligned} (\beta+\mathrm{i}\omega)^2 \left(\frac{F^{\text{discrete}}_{\text{steady}}}{R} - \frac{F^{\text{exact}}_{\text{steady}}}{R} \right) = \\ \left[\frac{1}{2}\xi\omega^2 - \mathrm{i}\beta\omega(\nu-1)(\xi-1)^2 \right. \\ \left. + \beta^2\{\mu_{1,I}\xi^2 + \mu_{1,II}(\nu-1)^2(\xi-1)^2\}\right]\Delta t \\ + O(\Delta t^2). \end{aligned} \tag{33}$$

Thus, it can be verified that, independently of ω and β, if $\nu = 0$ there is *a priori* no combination of $(\xi, \mu_{1,I}, \mu_{1,II})$ that increases the accuracy of the discrete solution to $O(\Delta t)$. For the situation of the AAA-imp model, i.e.

$$(\phi_1^{1,I} + \phi^{2,I}) \mapsto \mathcal{D}^{\exp} \mapsto \mathcal{D}^{\text{imp}}, \tag{34}$$

(33) becomes

$$\left(\beta^2 + \frac{\omega^2}{2}\right)\Delta t + O(\Delta t^2).$$

An obvious alternative to (34) would be to couple the physics parametrization after the explicit part of the dynamics:

$$\mathcal{D}^{\exp} \mapsto (\phi_1^{1,II} + \phi^{2,II}) \mapsto \mathcal{D}^{\text{imp}}. \tag{35}$$

This scheme has the same stability function as the AAA-imp model (Figure 2(b)). The ratio of the amplitude of the discrete steady-state response calculated with (35) to the exact one is then

$$\left| \frac{F^{\text{discrete}}_{\text{steady}}}{F^{\text{exact}}_{\text{steady}}} \right| = 1 + \beta\Delta t. \tag{36}$$

Thus the discrete solution produces the correct steady-state one if $\beta = 0$, i.e. when there is no damping term. This is in contrast with the AAA-imp case and indicates again that *inserting the implicit physics parametrizations after the explicit part of the dynamics ($\xi = 0$) leads to a more accurate treatment of the steady-state solution.*

4.2.2. *Forced response*

Applying a Taylor series expansion in terms of Δt of $F_{\text{A}}^{+} - F^{\text{exact}}_{\text{forced}}$ calculated for the IFS-imp and AAA-imp scheme ((32) and (34), respectively) leads to:

DOI: 10.1002/qj

- IFS-imp:

$$F_{\mathrm{A}}^{+} - F_{\mathrm{forced}}^{\mathrm{exact}} = \frac{\mathrm{i}R\Omega(kU - \mathrm{i}\beta + 2\omega + \Omega - \omega^{*})}{2(kU - \mathrm{i}\beta + \omega + \Omega)} \mathrm{e}^{\mathrm{i}(kx+\Omega t)} \Delta t^{2} + O(\Delta t^{3}), \tag{37}$$

- AAA-imp:

$$F_{\mathrm{A}}^{+} - F_{\mathrm{forced}}^{\mathrm{exact}} = -\mathrm{i}R \frac{(kU + \omega)^{2} + 2\beta(\beta + \mathrm{i}\Omega) - \omega\Omega - \Omega^{2} + \Omega\omega^{*}}{2(kU - \mathrm{i}\beta + \omega + \Omega)} \times \mathrm{e}^{\mathrm{i}(kx+\Omega t)} \Delta t^{2} + O(\Delta t^{3}). \tag{38}$$

Both schemes have the same formal accuracy ($O(\Delta t)$). However, IFS-imp is an order more accurate than AAA-imp for $\Omega = 0$, i.e. in the case of a stationary forcing, e.g. one caused by orography.

In order to study the impact of the forcing term in a general manner for $-\pi \leq \Omega\Delta t \leq \pi$, the maximum is now taken over the dimensionless parameters $\widetilde{U}$, $\widetilde{\omega}$ and $\widetilde{\Omega}$ for the two schemes corresponding to IFS-imp and AAA-imp.

The maximum ratio $|F_{\mathrm{A}}^{+}/F_{\mathrm{forced}}^{\mathrm{exact}}|$ of the amplitude of the approximate forced response to the exact one (Table III) is plotted in Figure 5.

This ratio can also be considered as an amplification factor $|\mathcal{A}|$ since:

$$\left| \frac{F_{\mathrm{A}}^{+}}{F_{\mathrm{forced}}^{\mathrm{exact}+}} \right| = \left| \frac{\mathcal{A}F_{\mathrm{A}}^{0}}{\mathrm{e}^{\mathrm{i}\Omega\Delta t} F_{\mathrm{A}}^{0}} \right| = |\mathcal{A}|. \tag{39}$$

For the resonant cases with $\beta = 0$ and $\omega + kU + \Omega = 0$, the forced resonant solution in Table III was taken for $F_{\mathrm{forced}}^{\mathrm{exact}}$ instead of the forced regular solution. Note that the ensemble of states from which the maximum is taken includes the states that were studied in Egger (2003) for the values $M = 1$ that are near resonance with $\beta\Delta t = 0$, $\omega\Delta t = \omega^{\star}\Delta t = 0$ in (2).

As is shown in Figure 5(a), for small $\beta\Delta t$ ($0 \leq \beta\Delta t \leq 2$), the amplification factor $|\mathcal{A}|$ of the IFS-imp scheme decreases monotonically as the damping coefficient increases. Thus as noted by SWC02b, the amount of vertical diffusion present plays an important role in damping spurious amplification of the numerical solution of the forced response. However, for large $\beta\Delta t$ ($\beta\Delta t \geq 2$), the amplification factor $|\mathcal{A}|$ increases with increasing $\beta\Delta t$, which is in agreement with Figure 2(a) where $|\mathcal{A}|$ starts to grow for $\beta\Delta t$ greater than 2. This is in contrast with the IFS-imp case (Figure 5(b)) which is less accurate and where the amplification factor $|\mathcal{A}|$ is approximately constant for $0 \leq \beta\Delta t \leq 2$ and increases with increasing $\beta\Delta t$ for $\beta\Delta t \geq 2$. Moreover, the discrete solution is an order of magnitude greater than the exact solution. The precise meaning of this with respect to the real model structures is presently unclear to us. This has to be studied in real model codes, as will be discussed in Section 5.

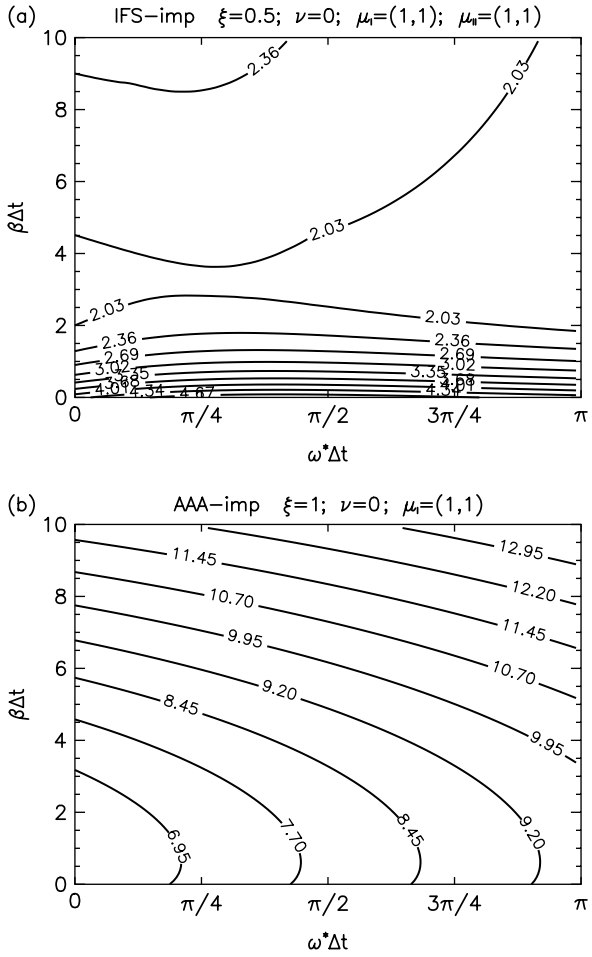

Figure 5. The ratio $|F_{\mathrm{A}}^{+}/F_{\mathrm{forced}}^{\mathrm{exact}}|$ of the amplitude of the approximate forced response, calculated (a) with (32) and (b) with (34), to the exact one (Table 3).

4.3. Physics calls as in SLAVEPP and AAA models

The aim of this section is to go one step further to mimic the situation of the real models.

The analysis presented in this section considers one diffusive process ($\phi^{1} \equiv -\beta F$) and two other forcing terms:

(i) $\phi^{2} \equiv R_1 \mathrm{e}^{\mathrm{i}(kx+\Omega_1 t)}$ which mimics the diurnal cycle of radiation in the real model with $\Omega_1 = 2\pi/86400$ and
(ii) $\phi^{3} \equiv R_2 \mathrm{e}^{\mathrm{i}(kx+\Omega_2 t)}$ which will represent one of the remaining forcings, with
- $\Omega_2 = 0.01$ for gravity wave drag.
- $\Omega_2 = 2\pi/3600$ for convection.
- $\Omega_2 = 2\pi/18000$ for clouds.

We introduce γ such that $R_1 = \gamma R_2$ and in order to separate the relative effect of the forcing amplitude, the maximum of the amplification factor $|\mathcal{A}|$ is taken over $\beta\Delta t$, between $[0, 2]$, and the dimensionless parameters $\widetilde{U}$ and $\widetilde{\omega}$.

The implicit schemes corresponding to IFS-imp, with the same order as given in Wedi (1999), and AAA-imp are respectively:

DOI: 10.1002/qj

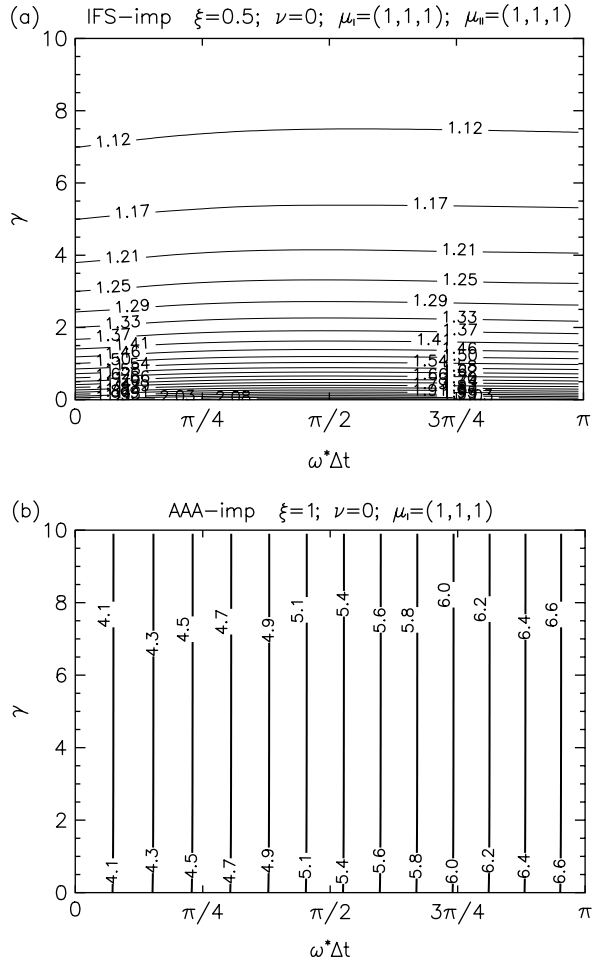

Figure 6. The ratio $|F_A^+/F_{\text{forced}}^{\text{exact}}|$ as a function of $\omega^*\Delta t$ and γ, calculated (a) from (40) and (b) from (41). ϕ^3 represents the gravity wave drag, but the results are the same for the other remaining forcings (convection or cloud).

- IFS:

$$\mathcal{D}^{\text{exp}} \mapsto \frac{1}{2}\Big\{(\phi_1^{2,II} \mapsto \phi_1^{1,II} \mapsto \phi_1^{3,II}) + (\phi_1^{2,I} \mapsto \phi_1^{1,I} \mapsto \phi_1^{3,I})\Big\} \mapsto \mathcal{D}^{\text{imp}}. \quad (40)$$

- AAA:

$$(\phi_1^{1,I} + \phi_1^{2,I} + \phi_1^{3,I}) \mapsto \mathcal{D}^{\text{exp}} \mapsto \mathcal{D}^{\text{imp}}. \quad (41)$$

The ratio $|F_A^+/F_{\text{forced}}^{\text{exact}}|$ of the amplitude of the approximated forced response, calculated with (40) and (41), to the exact one

$$F_{\text{forced}}^{\text{exact}} = \sum_{\alpha=1}^{2} \frac{R_\alpha}{\beta + \text{i}(\omega + kU + \Omega_\alpha)} \, \text{e}^{\text{i}(kx+\Omega_\alpha t)}, \quad (42)$$

is plotted in Figures 6(a) and (b) respectively as a function of $\omega^*\Delta t$ and γ. As can be easily verified, this ratio does not depend on R_1, R_2 but on γ only. In Figure 6, ϕ^3 represents the gravity wave drag, but the results are the same for the other remaining forcings (convection or cloud), i.e. independent of the specific value of Ω_2.

Figure 6 shows that

(i) for the IFS-imp scheme (Figure 6(a)), the ratio $|F_A^+/F_{\text{forced}}^{\text{exact}}|$ is practically independent of $\omega^*\Delta t$, decreases monotonically as γ increases and asymptotes to the exact value of unity for large value of γ;
(ii) For the AAA-imp scheme (Figure 6(b)) the ratio $|F_A^+/F_{\text{forced}}^{\text{exact}}|$ presents higher values, is independent of γ, and increases when increasing $\omega^*\Delta t$ between $[0, \pi]$.

Dubal *et al.* (2005) found that for realistic models, fast boundary-layer processes, such as turbulent diffusion, ought to be coupled implicitly at the end of the time step. In order to test this aspect with our simplified IFS model, a new scheme is assumed in which βF is treated at the end of the time step:

$$\mathcal{D}^{\text{exp}} \mapsto \frac{1}{2}\Big\{(\phi_1^{2,II} \mapsto \phi_1^{3,II} \mapsto \phi_1^{1,II}) + (\phi_1^{2,I} \mapsto \phi_1^{3,I} \mapsto \phi_1^{1,I})\Big\} \mapsto \mathcal{D}^{\text{imp}}. \quad (43)$$

The ratio $|F_A^+/F_{\text{forced}}^{\text{exact}}|$ of the amplitude of the approximated forced response, calculated with (43), to the exact one (42) is plotted in Figure 7.

From Figures 6 and 7, it would appear that a sequential splitting where the fast boundary-layer process, such as turbulent diffusion, is coupled last results in a scheme with reduced error and increased stability, having a ratio that is, for practical purposes, equal to 1.

It should be stressed that in the NWP models there are technical and scientific constraints that may prevent some reorganizations of the type from (40) to (43). For instance, as stated in Beljaars *et al.* (2004) on the recent version of the IFS model, vertical diffusion (represented by ϕ^1) should be called before convection (represented by ϕ^3) because the surface fluxes are needed for closure and the surface scheme is called from the vertical diffusion scheme. On the other hand, in the studied models there

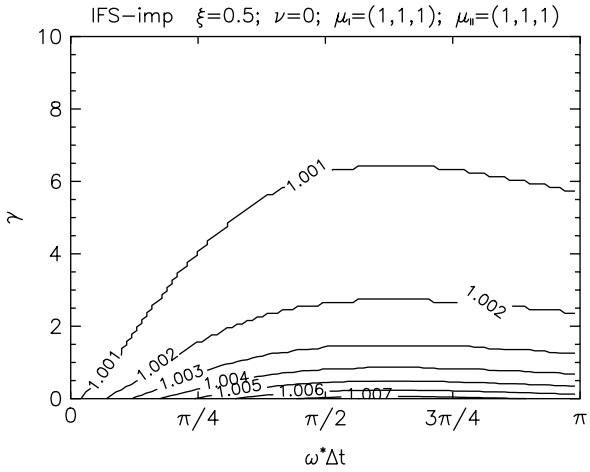

Figure 7. As Figure 6 but calculated from (43). ϕ^3 represents one of the remaining forcings (gravity wave drag, convection, or cloud).

DOI: 10.1002/qj

is for instance a numerical horizontal diffusion (see e.g. Váňa, 2003). It will be investigated in a subsequent study if this could play the role of ϕ^1 in (43).

This result suggests that, contrary to the stability analysis in Section 4.1, adapting the AAA time-step organization to the SLAVEPP structure does indeed improve stability.

5. Discussion and conclusions

The generalized framework introduced by Staniforth, Wood and Côté to study numerical aspects of coupling physics to dynamics has been extended in three ways:

(i) to consider the fact that the atmospheric state, quantified by ω, may differ from the reference state, quantified by ω^*, allowing to study the interaction of the physics – dynamics interface with the real atmospheric state,
(ii) to treat the analysis in a numerical way by taking the maxima over the variables that are not of interest, such as
(iii) to facilitate the treatment of the time-step organization of spectral models.

This extended framework is then used to make a comparison between two existing structures. The first option is the SLAVEPP scheme that was developed for the global IFS model of ECMWF. The second approach is the one of the ARPEGE model of Météo-France and its related limited-area model ALADIN of the ALADIN partners, and more lately in the newly developed non-hydrostatic AROME model of Météo-France. The properties of both methods were examined, first with regard to the free solution of the enhanced canonical problem and then in the context of a multiple forcing terms. Aspects of each of the coupling strategies are summarized below:

- The implicit AAA coupling has the advantage of being stable up to values of at least $\beta\Delta t = 10$. It does however have the drawback that it is only $O(\Delta t)$ accurate. It also corrupts the steady state. In the case of two forcing terms, the ratio of the amplitude of the approximated forced response to the exact one is independent of the forcing amplitude. Thus inserting a new forcing term into the time-step organization does not influence its accuracy.
- The idealized SLAVEPP coupling as represented by the IFS-imp structure in the present paper has the advantage of being second-order accurate and gives the correct representation of the exact steady-state response, but suffers from the disadvantage that the time step is limited by the stability condition, which is very restrictive for fast processes. The stability is however guaranteed by not averaging the diffusive processes along the SL trajectory as has been done in the implemented version of the ECMWF model (Beljaars *et al.*, 2004). Also, it is found within the present idealized IFS-imp framework (and without considering technical and scientific constraints), that in the case of two forcing terms, a sequential splitting where the fast boundary-layer process (such as turbulent diffusion or a horizontal diffusion) is coupled last results in a scheme with reduced errors and increased stability.
- It comes as a surprise that by treating the physics in a semi-implicit manner before the explicit part of the dynamics in the AAA frame yields the same properties as the IFS frame: (i) second-order accuracy of the diffusive processes and (ii) the same stability (compare Figures 4 and 2(a)). This amounts to a less drastic change of the code, since the time-step organization does not change but only the parametrization. However, concerning the role of the diffusive processes in the steady-state solution, the SLAVEPP approach still gives a better accuracy than the AAA approach.
- Inserting the physics after the explicit part of the dynamics in the AAA models leads to a more accurate treatment of the steady-state solution for a forcing without diffusive processes. Since the AAA models also comprise a climate version of ARPEGE, it might be useful to consider such a physics coupling in the AAA context to have a reduced climate drift.
- The results of the stability analysis, either in the case of singular diffusive physics or that of diffusion together with at least one forcing, lead to opposite conclusions concerning the superiority of one or the other scheme. The first analysis suggest that nothing will be gained if the time step of the AAA models is reorganized to the structure of the IFS models, while the latter suggests that *if* the diffusive process is coupled after the forcings in the IFS structure then the spurious amplification of the modes decreases (in agreement with Dubal *et al.* (2005)). One could argue that from all possible forcings *at least* radiation is always present. So the conclusion from the latter should be accepted; a reorganisation of the AAA code structure is expected to pay off.
- Figures 5(b) and 6(b) show some amplifications of an order of magnitude larger than the exact solution in the AAA structure, which is paradoxically in disagreement with the realistic behaviour of the real models. One explanation could be that in the real models the physics forcings have been developed within and thus adapted to the then-present time-step organization. Performing tests in a version of the AAA models that can both be run with the current time step and the SLAVEPP structure might shed light on this.

It should be noted that in the realistic models vertical diffusion is most often treated in an over-implicit way to avoid nonlinear instabilities (Bénard *et al.*, 2000). This kills the second-order accuracy in both the AAA models and in IFS which in practice runs with $(\xi, \nu, \mu_I, \mu_{II}) = (1/2, 0, 3/2, 3/2)$ not satisfying the accuracy condition in (23). Because of its nonlinear character, the precise consequences of this have to be studied in a broader context

DOI: 10.1002/qj

than this extended SWC framework. An alternative could be offered by the recently proposed scheme by Diamantakis *et al*. (2006). This scheme provides a possibility for an implicit, unconditionally stable treatment of vertical diffusion with increased accuracy. As such it is more apt to be fitted within the presented analysis.

Notwithstanding its simplicity, the Staniforth – Wood – Côté framework provides a good testing ground to probe into the possibilities of reorganizing the time step. The differences in the conclusions in Sections 4.1 and 4.3 show that the properties of the physics – dynamics coupling can not be studied by analysing the different physics parametrizations separately.

The presented framework for examining the numerics of physics – dynamics coupling is fairly general and could be adapted for other applications. The authors are currently exploring them. Possible applications for the AAA structure would be to examine the impact of computing the physics and the dynamics in a parallel manner and the role of over-implicit diffusive processes. Finally, the numerical analysis framework presented here could also be adapted to study iterative schemes such as, for instance, the ones in Bénard (2003). All of this lies beyond the scope of the present article and will be addressed in a subsequent publication.

Acknowledgements

We thank Jean-François Geleyn for encouraging us to perform this study and providing much useful input. We also thank Pierre Bénard, Jozef Vivoda and Filip Váňa for useful discussions during the various stages of this work. We thank the two anonymous reviewers. Their numerous comments were invaluable in substantially improving the presentation of this rather complex matter. This work is financed by the Belgian Science Policy unit, research project MO/34/013.

References

ALADIN International team. 1997. The ALADIN project: Mesoscale modelling seen as a basic tool for weather forecasting and atmospheric research. *WMO Bull.* **46**: 317–324.

Beljaars A, Bechtold P, Kohler M, Morcrette J-J, Tompkins A, Viterbo P, Wedi N. 2004. 'The numerics of physical parameterisation.' Pp 1–22 in Proceedings of the ECMWF seminar on Recent developments in numerical methods for atmospheric and ocean modelling. ECMWF, Reading, UK.

Bénard P. 2003. Stability of semi-implicit and iterative centered-implicit time discretizations for various equations systems used in NWP. *Mon. Weather Rev.* **131**: 2479–2491.

Bénard P, Marki A, Neytchev PN, Prtenjak MT. 2000. Stabilization of non-linear vertical diffusion schemes in the context of NWP models. *Mon. Weather Rev.* **128**: 1937–1948.

Bubnová R, Hello G, Bénard P, Geleyn J-F. 1995. Integration of the fully elastic equations cast in the hydrostatic pressure terrain-following coordinate in the framework of the ARPEGE/Aladin NWP system. *Mon. Weather Rev.* **123**: 515–535.

Catry B, Geleyn J-F, Tudor M, Bénard P, Trojáková A. 2007. Flux-conservative thermodynamic equations in a mass-weighted framework. *Tellus A* **59**: 71–79.

Caya A, Laprise M, Zwach P. 1998. Consequences of using the splitting method for implementing physical forcings in a semi-implicit semi-Lagrangian model. *Mon. Weather Rev.* **126**: 1707–1713.

Diamantakis M, Wood N, Davies T. 2006. An improved implicit predictor–corrector scheme for boundary layer vertical diffusion. *Q. J. R. Meteorol. Soc.* **132**: 959–978.

Dubal M, Wood N, Staniforth A. 2004. Analysis of parallel versus sequential splittings for time-stepping physical parameterizations. *Mon. Weather Rev.* **132**: 121–132.

Dubal M, Wood N, Staniforth A. 2005. Mixed parallel-sequential schemes for time-stepping multiple physical parameterizations. *Mon. Weather Rev.* **133**: 989–1002.

Dubal M, Wood N, Staniforth A. 2006. Some numerical properties of approaches to physics–dynamics coupling for NWP. *Q. J. R. Meteorol. Soc.* **132**: 27–42.

Egger J. 2003. Advection equation with oscillating forcing: numerical aspects. *Mon. Weather Rev.* **131**: 984–989.

Grabowski WW, Smolarkiewicz PK. 1996. Two-time-level semi-Lagrangian modeling of precipitating clouds. *Mon. Weather. Rev.* **124**: 487–497.

Hortal M. 1991. 'Formulation of the ECMWF model'. Pp 261–280 in Proceedings of the ECMWF seminar on numerical methods in atmospheric models. ECMWF, Reading, UK.

Lafore J-P, Stein J, Asencio N, Bougeault P, Ducrocq V, Duron J, Fischer C, Hreil P, Mascart P, Masson V, Pinty J-P, Redelsperger J-L, Richard E, Vilà-Guerau de Arellano J. 1998. The Meso-NH Atmospheric Simulation System. Part I: Adiabatic formulation and control simulations. Scientific objectives and experimental design. *Ann. Geophys.* **16**: 90–109.

McDonald A. 1999. 'The origin of noise in semi-Lagrangian integrations'. Pp 308–334 in Proceedings of the ECMWF seminar on recent developments in numerical methods for atmospheric modelling; 7–11 September 1998. ECMWF, Reading, UK.

Robert AJ. 1969. 'The integration of a spectral model of the atmosphere by the implicit method'. Pp 19–24 of Proc. of the WMO–IUGG Symposium on NWP, Tokyo, 26 Nov–4 Dec 1968. Japan Meteorological Agency: Tokyo.

Simmons AJ, Hoskins B, Burridge D. 1978. Stability of the semi-implicit method of time integration. *Mon. Weather Rev.* **106**: 405–412.

Staniforth A, Wood N, Côté J. 2002a. Analysis of the numerics of physics–dynamics coupling. *Q. J. R. Meteorol. Soc.* **128**: 2779–2799.

Staniforth A, Wood N, Côté J. 2002b. A simple comparison of four physics–dynamics coupling schemes. *Mon. Weather Rev.* **130**: 3129–3135.

Váňa F. 2003. 'Semi-Lagrangian advection scheme with controlled damping – an alternative way to non-linear horizontal diffusion in a numerical weather prediction model'. PhD thesis (in Czech with extended French and English abstracts), Faculty of Mathematics and Physics, Charles University, Prague, Czech Republic.

Wedi NP. 1999. 'The numerical coupling of the physical parametrizations to the 'dynamical' equations in a forecast model'. Tech. Memo. 274, ECMWF, Reading, UK.

DOI: 10.1002/qj